Laser-micromachining silicon three-dimensional structures, tunnels, and cavities

B. Shen, M. Allard, S. Boughaba, R. Izquierdo, and M. Meunier

Abstract: A laser-micromachining technique has been developed to make tunnels and cavities in Si under SiO_2 or Si_3N_4 films. Based on the laser-induced Cl_2 etching of Si, and high chlorine Si/SiO_2 and Si/Si_3N_4 etch-rate ratios, tunnels with length of up to 3 mm and cavities of 100×100 μm^2 were successfully fabricated in SiO_2/Si bilayered samples. Similarly, cavities of 50×50 μm^2 were also fabricated in Si_3N_4/Si samples.

Résumé : Nous avons développé une méthode de micro-usinage par laser permettant la réalisation de tunnels et de cavités dans un substrat de Si, sous des couches de SiO_2 ou de Si_3N_4. Cette technique est fondée sur la gravure du Si par Cl_2 et exploite les valeurs élevées des rapports de sélectivité Si/SiO_2 et Si/Si_3N_4. Des tunnels de longueur allant jusqu'à 3 mm et des cavités de 100×100 μm^2 ont été usinés dans des échantillons bicouches SiO_2/Si. Des cavités de 50×50 μm^2 ont également été réalisées avec succès dans des substrats Si_3N_4/Si.

1. Introduction

Conventionally, silicon micromachining is achieved using the photolithographic process, followed by wet anisotropic etching or reactive ion etching (RIE) [1, 2]. While successfully evolving from microelectronic fabrication technologies, these conventional techniques have some inherent limitations, such as 2D patterning and, in the case of wet etching, a dependence on the crystallographic orientation of the substrates [1, 2]. When the sacrificial layer technique is used, complex multipatterning, multilayering processes and lift-off etching are involved [1, 2]. Laser micromachining, which has provoked great interests over the last decade [3], has none of these shortcomings but rather several benefits that make it an attractive alternative technique [4–6]. Here the laser micromachining of silicon refers to the laser-induced chlorine etching of silicon. Since it is a computer-controlled, truly three-dimensional (3D) process permitting maskless patterning, applications in the emerging field of microelectromechanical systems (MEMS) have been explored [7–10]. Two important aspects of the laser micromachining of silicon are the transparency of silicon dioxide (SiO_2) and silicon nitride (Si_3N_4) to the Ar^+ laser and the high chlorine Si/SiO_2 and Si/Si_3N_4 etch-rate ratios [11]. These properties permit silicon to be patterned under SiO_2 or Si_3N_4 layers, yielding buried structures. In this way, tunnels and cavities may be fabricated [11–13]. Such microstructures may be applicable to microfluidic devices and free-standing parts of MEMS. In this paper, after presenting our laser-micromachining system, we report on the laser-induced Cl_2 etching of bare Si and on the fabrication of tunnels and cavities on SiO_2/Si and Si_3N_4/Si bilayered samples.

Received September 11, 1995. Accepted December 18, 1995.

B. Shen, M. Allard, S. Boughaba, R. Izquierdo, and M. Meunier.[1] Groupe de Recherche en Physique et Technologie des Couches Minces, Département de Génie Physique, École Polytechnique de Montréal, P.O. Box 6079, Station « Centre Ville », Montréal, QC H3C 3A7, Canada.

[1] Author to whom all correspondence should be addressed. **Telephone**: (514) 340-4971; **FAX**: (514) 340-3218; **e-mail**: meunier@phys.polymtl.ca

2. Laser-micromachining system and experimental techniques

A schematic of the laser-micromachining system is shown in Fig. 1. It consists of a cw Ar^+ laser, an optical system that is used to project the laser beam into a stainless steel reaction cell, a gas distribution system, and computer-controlled *xyz* translation stages. The Ar^+ laser may be set to three operation configurations in terms of wavelength and laser output power; when working at 488 nm, 514 nm, and multiline modes, the laser provides maximum powers of 1.5, 2, and 5 W, respectively. The optical system comprises mirrors, a dual wavelength quarter-wave plate (for 488 and 514 nm), and a microscope with a long-working-distance objective (25X, 0.31 NA). The quarter-wave plate is used to eliminate the polarization effect on etched structures [14], although the improvement is limited for the multiline operation. A beam splitter is inserted in the beam path to permit an operator to monitor the etching process on a video screen.

The laser TEM_{00} beam, which was projected and focused by the optical system, entered the reaction cell through a quartz window to irradiate the substrate surface. The $1/e^2$ beam spot diameter at the focal plane of the microscope objective was measured using the knife-edge technique [15] and found to be 7 μm. The focus position could be adjusted by moving the *z*-direction translation stage so that the energy density at the surface could be modulated and controlled. The laser direct-writing is controlled by the *xyz* translation stages, with a maximum speed of 16 mm s^{-1} and a spatial resolution of 0.1 μm.

After pumping down to 10^{-3} Torr (1 Torr = 133.3 Pa), the reaction cell and the gas distribution tubes were purged using N_2 and Ar gases. The reaction cell could be heated to accelerate the outgassing. The cell was then filled with high purity (99.99%) Cl_2, at pressures ranging from 100 to 500 Torr. The silicon surface to be patterned was moved vertically (*z*-direction) to be set in the focal plane of the objective and the laser was

Fig. 1. A schematic of the laser-micromachining system.

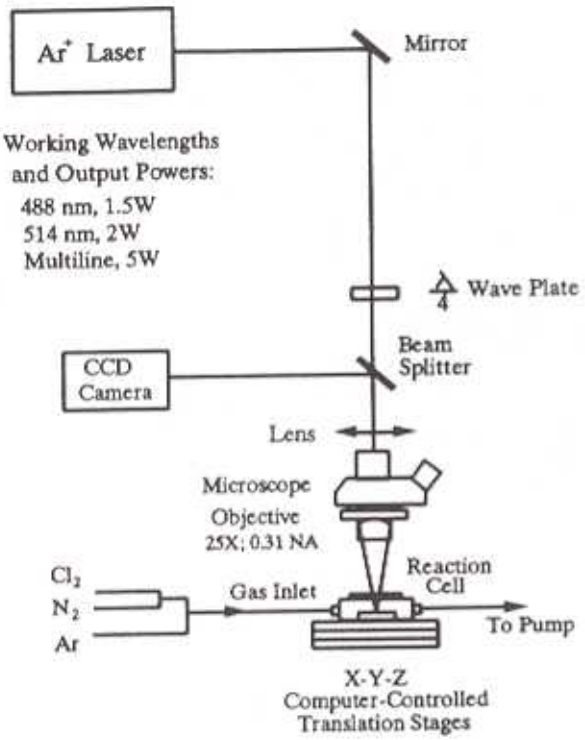

turned on at a sufficiently high power to heat the local surface to its melting temperature (1410°C). This melting threshold must be reached in the micromachining process to obtain the highest etching rates [6]. The localized melted zone defines a reaction area where the dissociation of the reactant chlorine molecules occurs. It must be emphasized that the dissociation of the chlorine molecules is pyrolytically controlled at the heated surface. No photolytic effect takes place in the gas phase where Cl_2 is almost totally transparent to the Ar^+ laser wavelengths [3]. The dissociation of the chlorine molecules results in the generation of free chlorine atoms (radicals) that react with the silicon to form volatile $SiCl_x$ ($x \geq 2$) compounds [6]. By moving the surface in the focal plane horizontally, the melted zone and, therefore, the etching can be displaced so that direct-writing patterns can be generated. The spatial resolution of the process almost corresponds to the dimension of the melted zone, which may be smaller than the beam spot size due to the Gaussian shape of the TEM_{00} beam [16–18].

Two sets of substrates were used. The first consisted of <100> Si wafers. These samples are first cleaned by successive immersing in hot trichloroethane (TCE), acetone, and isopropyl alcohol, then rinsed in deionized (DI) water. For the substrates on which the etching on bare silicon was investigated, the native oxide was removed using a 1:10 buffered HF solution for 30 s. After removal of the native oxide for the substrates on which the buried structures would be machined, dry oxidation (O_2–N_2 atmosphere, 1280°C) of silicon was carried out. SiO_2 films with thicknesses of 0.2 and 0.3 μm were grown. The second set consisted of silicon wafers covered with 0.7 μm thick PE-CVD Si_3N_4 films whose compositions have been verified to be stoichiometric (3:4), as measured by X-ray photoelectron spectroscopy (XPS). Note that silicon nitride films with 3:4 stoichiometry are transparent to Ar^+ laser [19]. The samples were cleaned using procedures similar to those mentioned above, except for the buffered HF-stripping step.

For etching beneath the SiO_2 or Si_3N_4 films, arrival and renewal of the Cl_2 gas at the reaction zone must be assured. Hence, prior to the introduction of the Cl_2 gas into the cell under vacuum, removal of the surface overlayer was performed using the Ar^+ laser beam to form an opening of 200×200 μm^2. Since the SiO_2 or Si_3N_4 films are transparent to the Ar^+ laser, the high-power beam was absorbed by the silicon substrate to form a molten layer that vaporized. The vaporization process may create a recoil pressure on the liquid layer and expel the molten silicon, which can break the overlayer leading to the removal of the SiO_2 or Si_3N_4 films. Another process that may play a role in this removal is the formation of volatile species, such as SiO, at high temperature. The direct-writing of the tunnels or cavities under the SiO_2 or Si_3N_4 was then carried out by moving the beam, which was initially focused on the bare silicon, from the exposed silicon surface toward the covered area.

A scanning electron microscope (SEM) was used to examine the etched structures, as well as to measure the etch depths.

3. Results and discussion

The preliminary experiments were performed on bare silicon substrates. The etch rate depends on the laser power, Cl_2 pressure, and scanning speed in a complex way. Figure 2*a* shows a SEM microphotograph of some grooves etched at a Cl_2 pressure of 500 Torr and a scanning speed of 100 μm s^{-1}. As the laser power of the 514 nm radiation was increased from 0.8 to 1.6 W, the grooves became deeper, varying from 0.4 to 8.1 μm. The width of these grooves correspondingly varied from 1.5 to 4.4 μm. Switching to the multiline operation mode, the same behavior was observed but, for powers beyond 3.2 W, did not result in greater depths. This may be seen in Fig. 2*b* where the dependence of the etch depth on the laser power is given for both operations. The increase in the etched depth with power, followed by saturation, may be related to the increase in the melted proportion of the irradiated silicon [20]. When a continuous, sufficiently thick, melted layer is obtained, no further increase in the depth is observed since any further increase of the beam energy will primarily contribute to latent heat [3, 21]. In the multiline operation mode, etch rates as high as 4×10^4 μm^3 s^{-1} were obtained. This value is comparable to that obtained in other studies [6, 7, 11].

The laser machining of buried structures was performed using 514 nm radiation. Laser powers ranging from 0.9 to 1.4 W, Cl_2 pressures of 100–500 Torr, and scanning speeds of 10–100 μm s^{-1} were used. Figure 3*a* shows a top view of tunnels etched under a 0.2 μm thick SiO_2 film at 500 Torr of Cl_2 and different scanning speeds and laser powers. These tunnels are 450 μm long and 3 μm wide. Tunnels of up to 3 mm long were also successfully obtained. Figure 3*b* shows an enlargement of the etching starting points in the initially ablated area. Starting at the exposed silicon surface, the etching is then displaced toward the SiO_2/Si area (to the left, in Fig. 3*b*). This adopted architecture permits the continued supply of Cl_2

Fig. 2. Etch-depth dependence on laser power at a Cl_2 pressure of 500 Torr. (*a*) SEM photograph of a group of grooves etched at a scanning speed of 100 μm s^{-1}, and 514 nm laser powers ranging from 0.8 to 1.6 W (from right to left). (*b*) Etch-depth dependence on laser power at 514 nm and multiline operation modes. Scanning speeds are 100 μm s^{-1} and 1 mm s^{-1}, respectively.

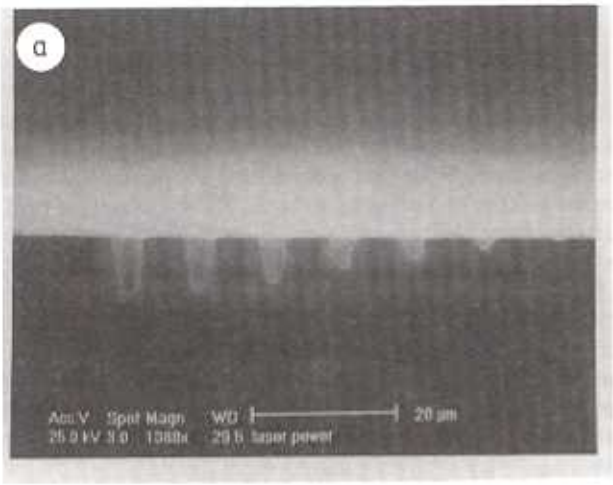

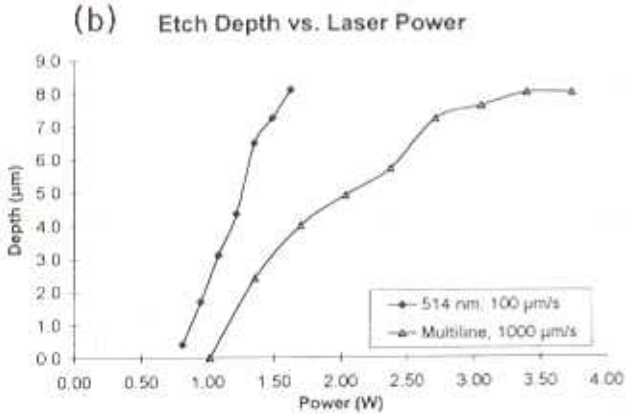

gas to the reaction zone. It must be emphasized that, even at a pressure of 100 Torr and a scanning speed of 100 μm s^{-1}, no evidence of gas transport limitation into the tunnels was observed. There is enough Cl_2 to sustain the reaction in tunnels as long as 450 μm. Indeed, by simply performing an additional etch starting at one of the previously machined tunnels, an additional interlinking of tunnels can be made, Fig. 3*b*. The SiO_2 film covering the tunnels was then carefully examined using high-resolution SEM, no physical defects were found in the overlayer, though the optical properties of the film need further characterization.

Figure 4 shows a cleaved sample in which two tunnels were etched under 0.2 μm thick SiO_2 at a laser power of 1.4 W, a Cl_2 pressure of 500 Torr, and scanning speeds of 10 μm s^{-1} (for the left tunnel) and 30 μm s^{-1} (for the right tunnel). The tunnels etched at 30 and 10 μm s^{-1} are 1.5 and 3.3 μm deep, and 2.6 and 2.8 μm wide, respectively.

By etching tunnels with several side by side paths (raster scan), with an overlap, it is possible to machine cavities. Figure 5 shows such a cavity of 100 × 100 μm^2 etched under a 0.2

Fig. 3. SEM microphotographs of tunnels under a SiO_2 film. (*a*) Tunnels etched in Si under 0.2 μm thick SiO_2 film.(*b*) Enlargement of (*a*) showing details of the starting points. Note that the first tunnel on the top is the result of double scans.

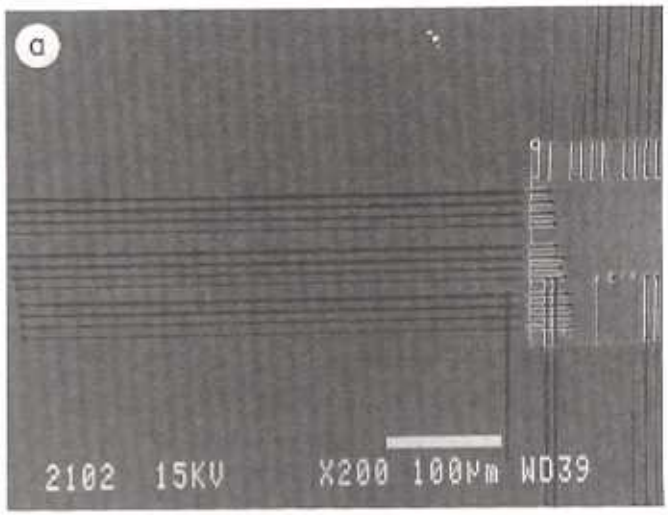

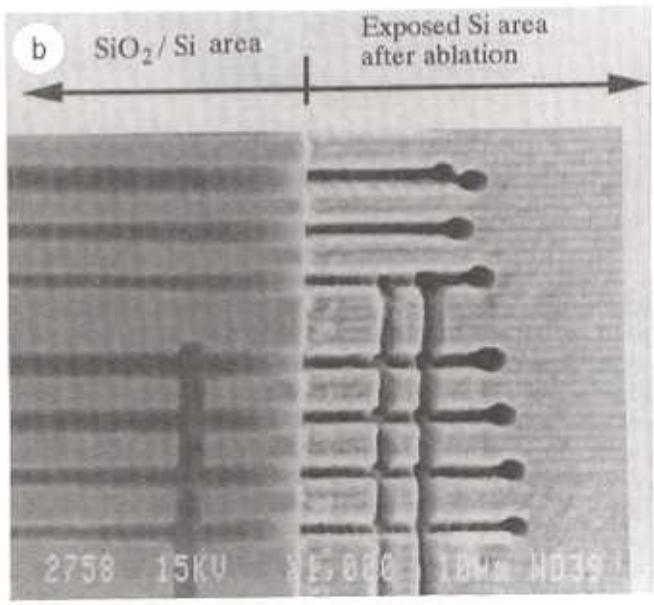

μm thick SiO_2 layer at a Cl_2 pressure of 500 Torr, a laser power of 1.2 W, and a scanning speed of 30 μm s^{-1}. The spacing between each tunnel is 2 μm. It took about 3 min to complete this fabrication. If higher scanning speed is used, the fabrication time could be shorter. The supply of the reactant gas to the machined area was provided through the tunnel connected at the top right corner of the cavity where the raster scanning started. This tunnel began at an ablated square area as that shown previously (Fig. 3), and was 1.6 mm long. Note that the gas supply to the etching area was not restricted by the turning point seen at the upper right corner of the cavity.

Since Si_3N_4 is a material whose mechanical properties are also of interest for MEMS [1], it is of interest for machine-buried structures under Si_3N_4 films. Figure 6 shows a cavity of 50 × 50 μm^2 etched in silicon under a 0.7 μm thick Si_3N_4 film. The scan started at the upper left corner, where a hole

Fig. 4. Cleaved SiO_2/Si sample showing two tunnels etched at 514 nm with a laser power of 1.4 W and a Cl_2 pressure of 500 Torr. Scanning speeds: 10 μm s^{-1} (left) and 30 μm s^{-1} (right). The cleavage was positioned close to the end of the tunnels, which are both 1.5 mm long.

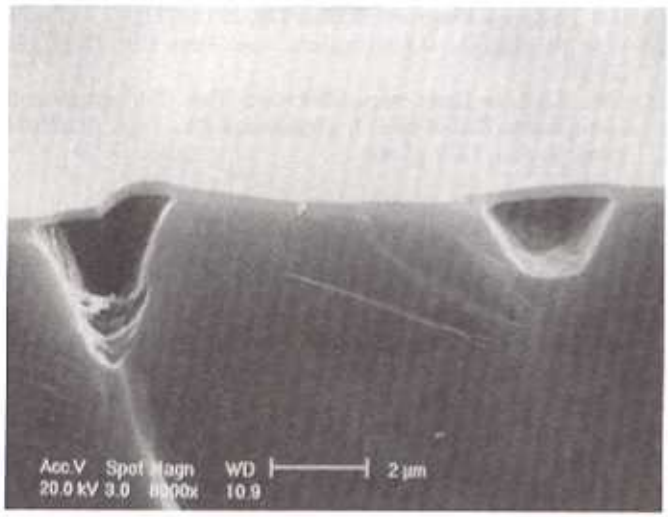

Fig. 5. SEM microphotograph of a cavity (100 × 100 $μm^2$) covered by a 0.2 μm thick SiO_2 film. The etching was carried out at laser power of 1.2 W, a Cl_2 pressure of 500 Torr, and a scanning speed of 30 μm s^{-1}.

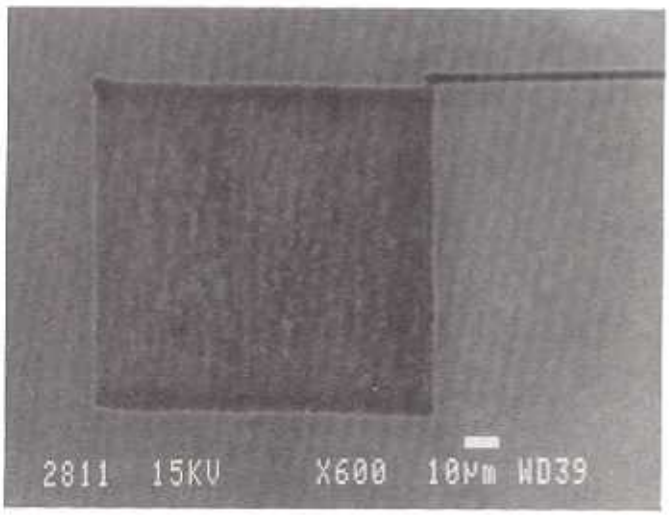

was first etched to supply the Cl_2 gas. The process was basically successful except that there is a small opening on one side of the square cavity. This may be due to the stress release of the Si_3N_4 film. Further investigations are in progress to avoid such imperfections.

4. Conclusions

Tunnels and cavities were successfully machined in silicon under SiO_2 films. No defects were observed in the SiO_2 overlayers. The use of Si_3N_4 instead of SiO_2 gave encouraging results.

Fig. 6. SEM microphotograph of a cavity (50 × 50 $μm^2$) covered by a 0.7 μm thick Si_3N_4 film. Laser power, 0.9 W; Cl_2 pressure, 100 Torr; and scanning speed, 100 μm s^{-1}.

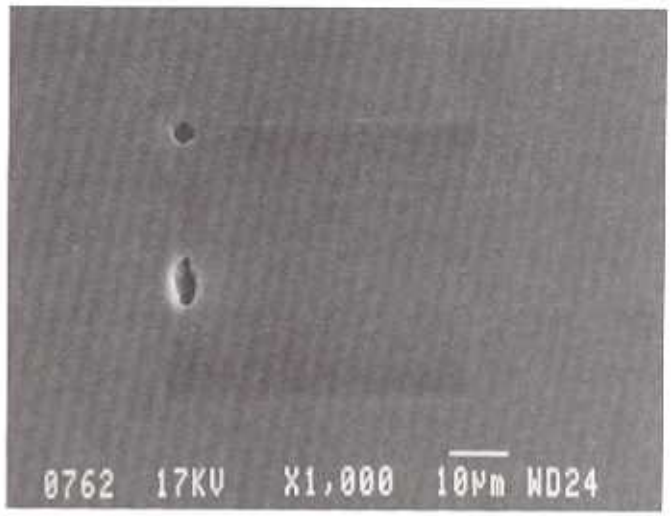

Laser micromachining is simple and more efficient because of its maskless approach and its truly 3D processing nature. This could be of interest for the fabrication of MEMS. Work is in progress on laser micromachining of microstructures involving tunnels, cavities, and sealed structures using laser deposition techniques [13].

Acknowledgments

The authors thank Mr. J.P. Lévesque for his technical assistance, and Mr. M. Caron and Mr. B. Hong for their SEM analyses. This work was supported by the Fonds pour la Formation de Chercheurs et L'Aide à la Recherche and funds from the Natural Science and Engineering Research Council of Canada.

References

1. K.E. Petersen. Proc. IEEE, **70**(5), 420 (1982).
2. C. Linder, L. Paratte, M-A. Gretillat, V.P. Jaecklin, and N.F. de Rooij. J. Micromech. Microeng. **2**, 122 (1992).
3. D.J. Ehrlich, R.M. Osgood, and T.F. Deutsch. Appl. Phys. Lett. **38**, 1018 (1981).
4. M. Müllenborn, H. Dirac, J.W. Petersen, and S. Bouwstra. *In* Transducers 1995: The 8th International Conference on Solid State Sensors and Actuators. p. 166.
5. D.J. Ehrlich. *In* Excimer lasers: The tool, fundamentals of their interactions with matter, field of application. *Edited by* L.D. Laude, Kluwer Academic Publishers, Netherlands. 1994. p. 307.
6. T.M. Bloomstein and D.J. Ehrlich. Appl. Phys. Lett. **61**(6), 708 (1992).
7. T.M. Bloomstein and D.J. Ehrlich. J. Vac. Sci. Technol. B, **10** (6), 2671 (1992).
8. M. Alavi, S. Buttgenbach, A. Schumacher, and H.-J. Wagner. Sens. Actuators A, **32**, 299 (1992).
9. M. Alavi, S. Buttgenbach, A. Schumacher, and H.-J. Wagner. *In* Transducers 91: IEEE International Conference on Solid State Sensors and Actuators. IEEE, New York. 1991. p. 512.
10. M. Alavi, Th. Fabula, A. Schumacher, and H.-J. Wagner. Sens. Actuators A, **37–38**, 661 (1993).
11. T.M. Bloomstein and D.J. Ehrlich. *In* Transducers 91: IEEE

International Conference on Solid State Sensors and Actuators. IEEE, New York. 1991. p. 507.
12. C. Arnone and G.B. Scelsi. Appl. Phys. Lett. **54**(3), 225 (1989).
13. B. Shen, R. Izquierdo, and M. Meunier. Proc. SPIE. **2045**, 91 (1993).
14. G.V. Treyz, R. Beach, and R.M. Osgood, Jr. J. Vac. Sci. Technol. B, **6**(1), 37 (1988).
15. Y.S. Liu. In Laser microfabrication: Thin film process and lithography. *Edited by* D.J. Ehrlich and J.Y. Tsao. Academic Press, Boston. 1989. p. 44.
16. Y.S. Liu. *In* Laser microfabrication: Thin film process and lithography *Edited by* D.J. Ehrlich and J.Y. Tsao. Academic Press, Boston. 1989. p. 27.
17. M. Müllenborn, H. Dirac, and J.W. Petersen. Appl. Phys. Lett. **66** (22), 3001 (1995).
18. M. Müllenborn, H. Dirac, and J.W. Petersen. Appl. Surf. Sci. **86**, 568 (1995).
19. H.R. Philipp. J. Electrochem. Soc. **120**, 295 (1973).
20. W.G. Hawkins and D.K. Biegelsen. Appl. Phys. Lett. **42**(4), 358 (1983).
21. I.W. Boyd. *In* Laser microfabrication: Thin film process and Lithography. *Edited by* D.J. Ehrlich and J.Y. Tsao. Academic Press, Boston. 1989. p. 566.